sustainability

MDPI

Article

Assessing Land Degradation Through Remote Sensing and Geospatial Techniques for Sustainable Development Under the Mediterranean Conditions

Elsherbiny A. Ali [1], Ahmed S. Elnagar [1], Nazih Y. Rebouh [2,*] and Mohamed E. Fadl [3,*]

[1] Geography Department, Faculty of Arts, Zagazig University, Zagazig 44519, Egypt; elsherbiny_ahmed@zu.edu.eg (E.A.A.); asmorsi@zu.edu.eg (A.S.E.)
[2] Department of Environmental Management, Institute of Environmental Engineering, RUDN University, 6 Miklukho-Maklaya St., Moscow 117198, Russia
[3] Division of Scientific Training and Continuous Studies, National Authority for Remote Sensing and Space Sciences (NARSS), Cairo 11769, Egypt
* Correspondence: n.yacer16@outlook.fr (N.Y.R.); madham@narss.sci.eg (M.E.F.)

Abstract

This study provides a comprehensive assessment of land degradation (LD) in Damietta Governorate, Egypt, by integrating multiple indices, including the Geology Index (GI), Topographic Quality Index (TQI), Physical Quality Index (PQI), Chemical Quality Index (CQI), Wind Erosion Quality Index (WEQI), and Vegetation Quality Index (VQI). The study findings reveal the following: (1) Soil quality shows moderate suitability for agricultural and developmental activities and can support productive land use with proper management (68.14% physical quality, 51.54% chemical quality), with 14.03–37.75% high-quality areas supporting intensive farming and 10.71–17.83% degraded soils requiring intervention; (2) nearly 31.83% of the area faces high degradation risk, particularly from wind erosion (27.41% high-risk areas), emphasizing the need for erosion control measures; and (3) vegetation analysis shows that 51.5% of land has inadequate cover (low/very low quality), highlighting restoration needs. The LD mapping reveals that 32.70% of the area is at low risk, 35.48% at moderate risk, and 31.83% at high to very high risk, underscoring the need for urgent restoration and sustainable land management practices. The study validates the effectiveness of ordinary kriging (OK) models in predicting soil properties, with tailored variogram models (Exponential, Spherical, and Gaussian) enhancing prediction accuracy. Overall, this study identifies statistically significant factors influencing LD in the study area, providing a data-driven foundation for sustainable land management, agricultural development, and environmental conservation.

Keywords: land degradation; geospatial techniques; soil quality indices; sustainable land management; quality Indices

check for updates

Academic Editors: Meriame Mohajane, Antonietta Varasano, Paola D'Antonio and Costanza Fiorentino

Received: 28 April 2025
Revised: 19 June 2025
Accepted: 24 June 2025
Published: 3 July 2025

Citation: Ali, E.A.; Elnagar, A.S.; Rebouh, N.Y.; Fadl, M.E. Assessing Land Degradation Through Remote Sensing and Geospatial Techniques for Sustainable Development Under the Mediterranean Conditions. *Sustainability* **2025**, *17*, 6087. https://doi.org/10.3390/su17136087

Copyright: © 2025 by the authors. Licensee MDPI, Basel, Switzerland. This article is an open access article distributed under the terms and conditions of the Creative Commons Attribution (CC BY) license (https://creativecommons.org/licenses/by/4.0/).

1. Introduction

Land degradation (LD) is an interactive worldwide environmental hazard with far-reaching implications. LD affects the ecosystems productivity capacity by depleting soil fertility, reducing vegetation cover, and weakening water retention and nutrient cycling processes [1]. LD changes undermine soil productivity, posing a major threat to food security, particularly in developing and dry regions that rely heavily on land resources for subsistence farming like Egypt [2]. Climate change, with rising temperatures, erratic

rainfall patterns, and more frequent extreme weather events, is leading to increased rates of desertification, soil erosion, and loss of fertile land. This not only affects agricultural productivity but also has broader social and economic impacts, including rural poverty and migration [3].

The LD has emerged as a critical global environmental challenge, with approximately 25% of the world's total land area already degraded according to recent United Nations Convention to Combat Desertification (UNCCD) estimates [4]. Remote sensing (RS) and geographic information systems (GIS) have become indispensable tools for monitoring these changes, offering spatially explicit data on vegetation cover and land use/land cover (LULC) dynamics [5]. Globally, three primary degradation processes dominate (1) soil erosion, affecting 1.43 billion hectares worldwide [1]; (2) salinization, impacting 20% of irrigated lands [6]; and (3) vegetation degradation, responsible for 23% of anthropogenic CO_2 emissions [7]. The Mediterranean region, including Egypt, shows particularly acute vulnerability due to climate change, with satellite data revealing an 18% increase in aridity index and potential evapotranspiration [8]. Recent advances in RS/GIS methodologies have revolutionized degradation monitoring [9]. Sentinel-2 data now enables 10 m resolution vegetation monitoring, while machine learning algorithms improve classification accuracy [10]. These earth platforms exemplify global efforts to standardize degradation assessments, aligning with Sustainable Development Goals (SDG 15.3) [11].

In Egypt, unsustainable agricultural practices, such as over-irrigation, improper drainage, and excessive use of chemical fertilizers, have led to soil salinization and waterlogging, degrading limited fertile lands, in addition, urban encroachment on agricultural lands has reduced the availability of productive soil [12]. Damietta Governorate, Egypt, is known for its fertile soils and agricultural activities, and it plays a vital role in Egypt's agricultural output and coastal ecosystems; however, the governorate is increasingly vulnerable to LD due to intensive farming practices, rapid urbanization, and the impacts of climate change, such as rising sea levels and saltwater intrusion [13].

Assessing LD in Egypt is essential for developing effective mitigation and adaptation strategies, using RS and GIS techniques as powerful tools for monitoring LD, which provide spatially and explicit data such as vegetation cover, soil quality, and LULC changes. Therefore, previous studies have highlighted the severity of LD in Egypt using RS and GIS approaches, with significant areas of the Nile Delta experiencing salinization and reduced fertility [14]. One of the strengths of RS and GIS is its ability to integrate geospatial data from diverse sources, including satellite imagery, field surveys, and climate models, this multi-source approach enhances the accuracy and comprehensiveness of LD assessments [15,16], and GIS has been used to map soil salinity in the Nile Delta, where irrigation with saline water and poor drainage systems have led to the accumulation of salts in the soil [17]. Mohamed et al., 2013 [18], using GIS and RS techniques to evaluate the spatial distribution of soil salinity in the Nile Delta, Egypt, revealed that over 30% of the region's agricultural land is affected by salinity; these findings have informed the implementation of sustainable land management practices, such as the use of salt-tolerant crops and improved irrigation. The rapid urbanization in Egypt has led to the conversion of fertile agricultural lands into built-up areas, and GIS-based LULC change detection studies have quantified the loss of arable land in the Nile Delta and surrounding regions, highlighting the need for stricter land use regulations [19].

Previous studies have demonstrated the effectiveness of RS and GIS in monitoring LD in various regions. For example, research conducted in the Nile Delta region of Egypt has utilized satellite imagery and geospatial analysis to assess changes in land use and land cover, revealing significant losses of agricultural land due to urbanization and soil salinity [20–22].

In the context of Damietta Governorate, limited but relevant studies have been conducted to assess environmental changes and LD. For instance, research by El-Gammal et al., 2015 [23], used RS and GIS to analyze land use changes in the Nile Delta, including Damietta, and found significant losses of agricultural land due to urban expansion. Another study by El-Zeiny et al., 2016 [24], focused on the impacts of climate change on coastal areas in Damietta, highlighting the risks of saltwater intrusion and its effects on soil quality and agricultural productivity. These studies underscore the urgent need for comprehensive monitoring and management of LD in Damietta, particularly in light of the region's unique ecological and socio-economic characteristics.

While existing studies have applied RS/GIS to assess LD in Egypt's Nile Delta, critical limitations remain: (1) Most prior work focuses on broad-scale delta-wide assessments, neglecting localized drivers and mitigation strategies for high-risk subregions like Damietta Governorate, a key agricultural and coastal zone facing compounded pressures from soil salinization, erosion, and urbanization; (2) Current methods often prioritize single indicators (e.g., NDVI for vegetation), lacking integrated frameworks that simultaneously evaluate geological, chemical, physical, and anthropogenic factors; and (3) Few studies leverage spatio-temporal data with geostatistical modeling to quantify degradation rates and project future risks under climate change scenarios. This study fills these gaps by introducing a spatially explicit, multi-index approach tailored to Damietta's unique coastal-agricultural system, linking diagnostic assessments with targeted conservation planning.

This study aims to employ advanced RS and geospatial techniques to monitor and assess LD dynamics in Damietta Governorate (northeastern Nile Delta, Egypt), under Mediterranean conditions, to inform sustainable land management strategies by analyzing multi-temporal satellite imagery (2024), geospatial data, and the methodological framework, which integrates spectral indices, soil analysis, land cover classification, and geostatistical modeling to quantify degradation factors based on (1) identifying the areas that experience LD, (2) assessing the driving factors and processes contributing to LD, and (3) providing actionable insights for mitigating LD impacts in the investigated area. The study results will contribute to the development of evidence-based strategies for sustainable land use and environmental conservation in the investigated area.

2. Materials and Methods

2.1. Description of the Study Area

Damietta Governorate is a strategically significant region located in the northeastern part of the Nile Delta in Egypt. It is uniquely positioned as a peninsula, bordered by Dakahlia Governorate on its southern, western, and eastern sides, while its northern boundary overlooks the Mediterranean Sea. To the east, the governorate is flanked by Manzala Lake, one of the largest coastal lakes in Egypt, which covers approximately 20% of Damietta's total area. Damietta Governorate lies between the geographical coordinates of 31°28′29″ to 32°03′32″ E longitude and 31°09′28″ to 31°31′45″ N latitude (Figure 1). It spans an area that represents about 4.7% of the Nile Delta region and approximately 1.22% of Egypt's total land area. Its proximity to the Mediterranean Sea and its location within the fertile Nile Delta make it a critical area for agriculture, fisheries, and trade, while also exposing it to environmental challenges such as saltwater intrusion, coastal erosion, and land degradation. The topography of Damietta Governorate is relatively flat, which is characteristic of the Nile Delta region, with elevations ranging from sea level to a few meters above (Figure 2). Soil classification order in Damietta area was *Entisols*, with three sub orders: *Typic torrifluvents*, *Typic torripsamments*, and *Typic psamaquents*, according to soil survey staff [25]. Agricultural land constitutes the majority of Damietta area, which covered

approximately 50,000 hectares (ha), and the alluvial soils of the River Nile are generally deep due to the gentle topographic nature of the River Nile and its flood plain [26].

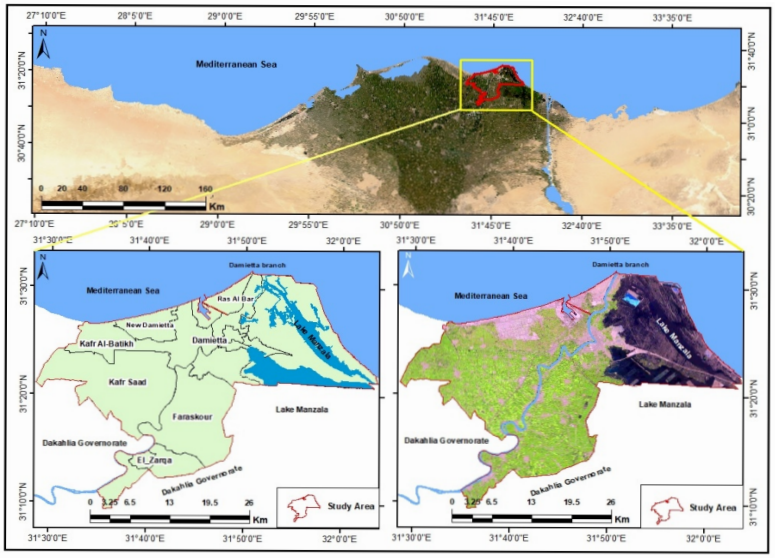

Figure 1. Location map of the study area, based on Landsat-8 (bands; B4, B3, and B2).

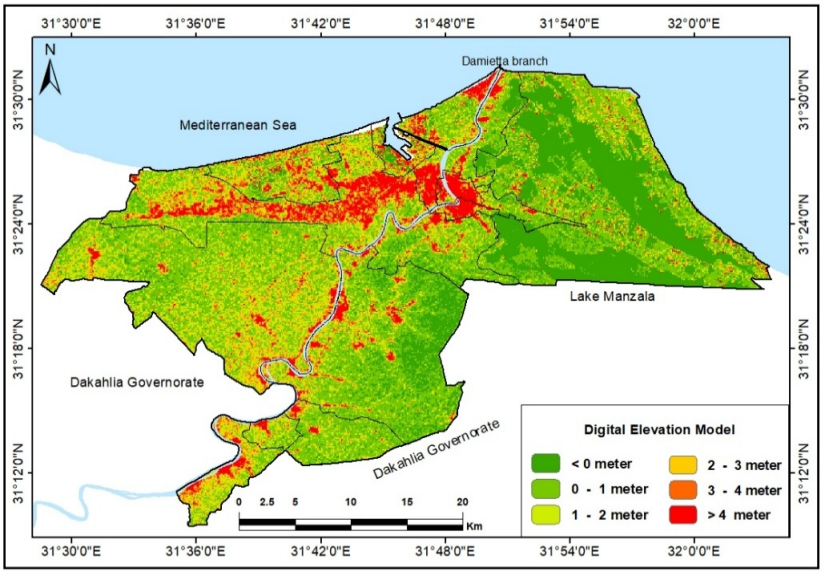

Figure 2. Digital Elevation Model (ASTER-DEM) of the study area.

2.2. Land Use/Land Cover

Damietta governorate is characterized by a mix of agricultural lands (60% of the area), urban and built-up areas (15%), wetlands and water bodies (20%, including the Nile branches and Lake Manzala), and bare land (5%). The northern coastal zone features dynamic natural landscapes, including sandy beaches, dunes, and marine areas, while the eastern side is dominated by the brackish waters of Manzala Lake—an ecologically important wetland, which is separated from the Mediterranean Sea by a narrow sandbar.

2.3. Climate of the Study Area

Damietta governorate experiences a Mediterranean climate, characterized by hot, dry summers and mild, wet winters, as shown in Table 1 and Figures 3 and 4. The average annual precipitation/rainfall in the study area during the period (1991–2022) is relatively low, with an annual precipitation ranging between 100 and 200 mm, and the average

monthly precipitation/rainfall during this period was approximately 12.08 mm, with the most precipitation occurring between October and March. Temperatures typically range from 14.6 °C in winter to 31.6 °C in summer, and the average annual temperature in the study area is 20.5 °C, with occasional heatwaves during the summer months. The region is also influenced by coastal winds and sea breezes, which moderate temperatures but can contribute to soil erosion and salt spray.

Table 1. Meteorological data of the study area during the period (1991–2022).

	Avg. Temperature (°C)	Min. Temperature (°C)	Max. Temperature (°C)	Precipitation/ Rainfall (mm)	Humidity (%)	Rainy Days (d)
January	14.6	11.6	17.9	38	63	6
February	14.9	11.7	18.4	29	63	5
March	16.6	13.2	20.6	15	63	2
April	18.8	15.1	22.9	6	65	1
May	21.9	18	26.2	1	66	0
June	25	21.3	29.2	0	68	0
July	26.9	23.3	31.2	0	70	0
August	27.4	23.9	31.6	0	70	0
September	26.2	22.9	30	0	66	0
October	23.7	20.7	27.2	9	65	1
November	20.4	17.7	23.5	18	63	3
December	16.7	13.9	19.8	29	62	4
Average	20.5	17.7	24.8	12.08	65.3	1.8

Source: [National Oceanic and Atmospheric Administration (NOAA), 2023 report; https://www.ncei.noaa.gov/access/monitoring/monthly-report/global/202213, accessed on 27 April 2025].

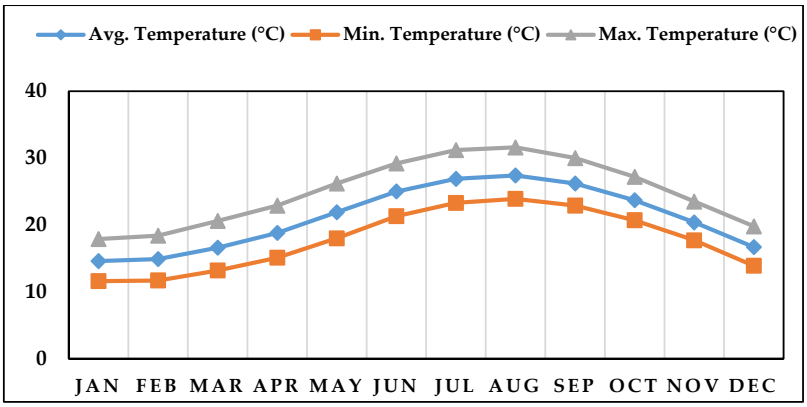

Figure 3. The annual average, maximum, and minimum temperature in the study area during the period (1991–2022).

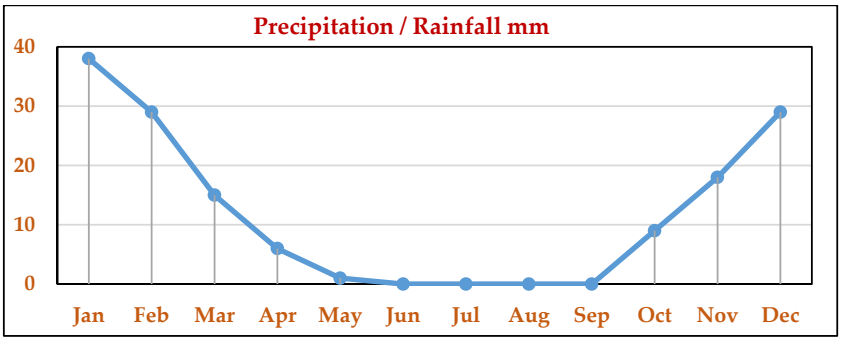

Figure 4. The monthly amount of precipitation in the study area during the period (1991–2022).

2.4. Geological Formation of the Study Area

The geological formation of Damietta Governorate (Figure 5) is the result of complex geological processes over an extended period, primarily shaped by the dynamic interaction between the Nile Delta's progradation and marine erosion [27]. Progradation, driven by the Nile's sediment load during periods of lower sea levels, is influenced by factors such as water discharge, sediment supply, and the configuration of Nile distributaries. Conversely, marine erosion, facilitated by waves, currents, and tidal flows, disperses sediments, while additional factors such as wind and sea level changes have also played significant roles in shaping the region. The area is predominantly flat, characterized by Nile silt, stabilized sand dunes, and active dunes. Stabilized dunes, low and vegetated with reddish sand, dominate the islands of nearby Manzala Lake, while active dunes, reaching heights of 2–3 m, are sharper and more pronounced. The interdune areas feature sabkha deposits, consisting of dark gray to gray silt layers with abundant vegetation roots. The shoreline spans approximately 8.3 km from east to west. However, recent land reclamation, urbanization, and beach replenishment projects have significantly reduced the extent of dunes and sabkha, with vast sand areas being repurposed for development and coastal restoration.

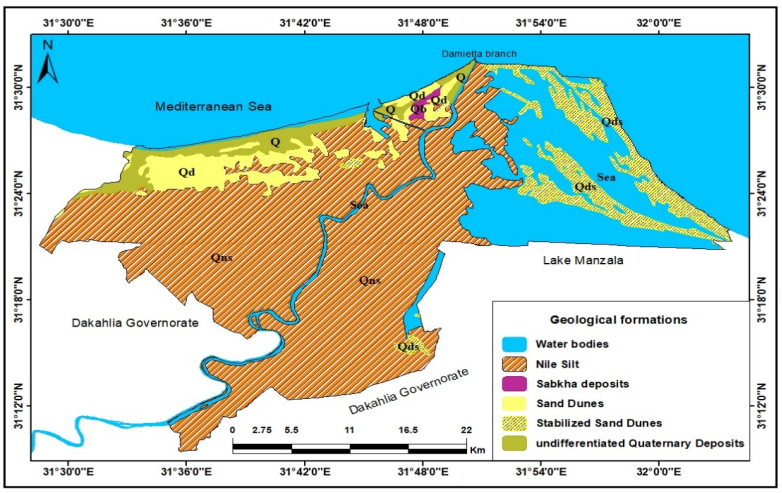

Figure 5. Geological map of the study area, based on the geological map of Egypt, [27].

Figure 6 illustrates the methodology employed in this study and highlights key stages, such as data collection, analysis, model application, and validation, ensuring a systematic and transparent approach to achieving the study's objectives.

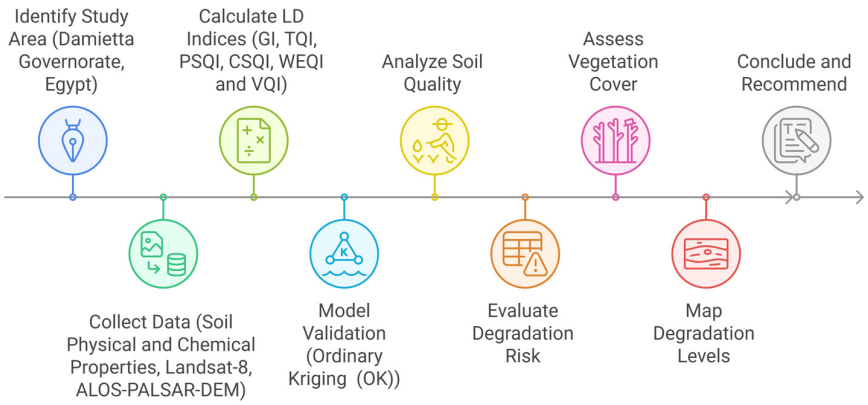

Figure 6. The proposed methodology flowchart.

2.5. Samples Collection and Analysis

Collecting soil samples is an important step in assessing soil quality and exploring and knowing its physical and chemical properties. A field study was conducted during October 2024, and then twenty-five geo-referenced soil profiles were distributed using a stratified random sampling approach to ensure representation across (a) key soil types, (b) land use/cover gradients, (c) topographic positions (slope, aspect, elevation), and (d) visible degradation gradients created due to a 150 cm depth or lithic contact. Sampling locations were georeferenced (Figure 7) to cover the study area systematically and distributed over the study area. Sampling locations were stratified to cover (1) dominant geological formations (Nile silt, sand dunes, and sabkha deposits), (2) major land use/cover types (agricultural, urban, and bare degraded areas), (3) topographic variability (elevation gradients, slope aspects, and low-lying coastal zones), and (4) observable degradation severity (from stable vegetated areas to eroding or saline hotspots). This approach aligns with FAO [28] guidelines for soil health assessment in deltaic regions and addresses the limitations of purely random sampling by systematically capturing critical soil-forming factors. Sixty-five soil samples were collected from the subsequent horizons and transported to the laboratory. Undisturbed 100 cm^3 volume soil cores were collected at each depth to determine soil bulk density (BD). Three replicates of 1 kg each were combined into a composite sample, stored in polyethylene sacks. The samples were air-dried, ground, sieved through a 2 mm mesh, and prepared for analyses. Soil analyses followed the Soil Survey Staff [29] guidelines. Particle size distribution was determined using the standard pipette method, while soil pH and electrical conductivity (EC) were measured in the 1:2.5 soil-water suspension and soil paste extract, respectively. Soil Organic matter (OM) was quantified using the Walkley–Black procedure, and calcium carbonate content was determined with a calcimeter, and gypsum content was assessed using the acetone precipitation method, as summarized in Table 2.

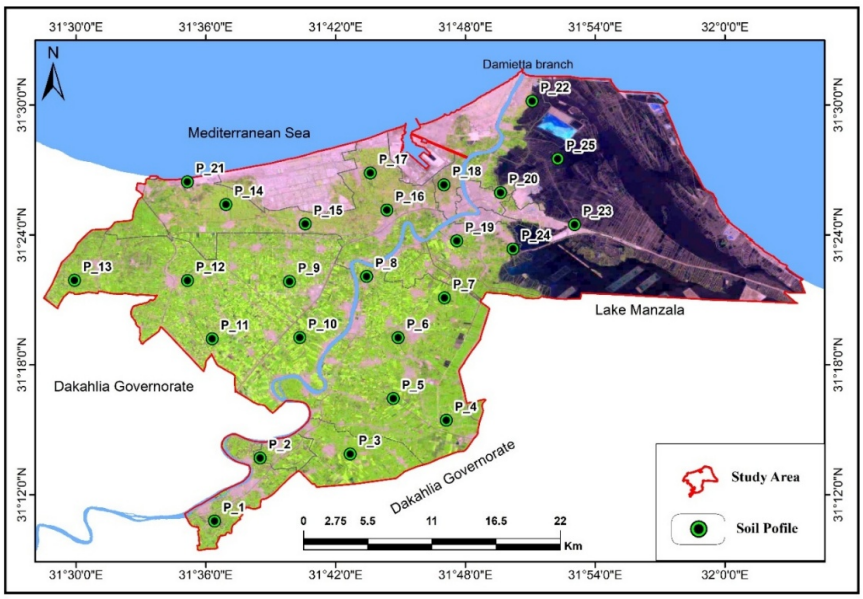

Figure 7. Landsat-8 satellite image based on B4, B3, B2 bands, showing the distribution of soil profiles in the study area by (GPS).

Table 2. Chemical and physical characteristics of the study area soils.

Profile	Land Unit	Texture	Sand (%)	Silt (%)	Clay (%)	pH	EC (ds/m)	Bulk Density (g/cm^3)	$CaCO_3$ (%)	OM (%)
1	Cultivated land	Clay loam	18	45	37	8.01	2.10	1.23	2.11	0.29
2	Cultivated land	Clay	12	17	71	7.34	2.91	1.27	1.85	0.31
3	Cultivated land	Clay	12	24	64	8.15	2.79	1.34	1.24	0.30
4	Cultivated land	Clay loam	18	45	37	8.21	3.01	1.42	1.13	0.47
5	Cultivated land	Clay	12	17	71	8.32	1.76	1.26	2.03	0.78
6	Cultivated land	Clay	12	24	64	8.67	1.88	1.52	2.28	0.61
7	Cultivated land	Clay loam	19	46	35	7.91	2.56	1.28	2.64	0.80
8	Cultivated land	Clay	17	22	61	7.79	1.95	1.33	0.54	0.74
9	Cultivated land	Clay loam	14	27	59	8.67	2.64	1.57	1.42	0.52
10	Cultivated land	Clay	12	23	65	7.58	1.73	1.46	0.52	1.34
11	Cultivated land	Clay loam	21	46	33	8.01	3.01	1.40	2.14	0.82
12	Cultivated land	Clay loam	15	46	39	7.15	3.44	1.22	2.42	1.12
13	Cultivated land	Clay loam	19	47	34	7.56	2.78	1.56	2.34	1.03
14	Cultivated land	Sand	83	7	10	8.21	2.80	1.01	1.89	1.34
15	Cultivated land	Sand	79	12	9	8.11	3.01	1.91	0.87	0.64
16	Cultivated land	Sand	87	8	5	8.34	3.22	1.20	2.09	2.10
17	Cultivated land	Sand	79	12	9	7.89	1.56	1.03	2.33	1.36
18	Cultivated land	Sand	75	16	9	8.32	2.56	1.37	1.36	1.56
19	Cultivated land	Clay loam	19	48	33	7.45	1.23	1.27	1.98	1.64
20	Sabkha	Loamy sand	66	31	3	7.65	20.21	1.53	2.67	1.27
21	Sabkha	Sand	88	7	5	8.42	17.66	1.63	0.57	0.98
22	Lake shore	Sand	87	7	6	8.89	22,89	1.76	2.90	0.81
23	Lake shore	Sand	78	13	9	8.01	32.17	1.35	3.72	1.34
24	Lake shore	Sandy loam	81	11	8	8.76	39.32	1.65	1.67	0.97
25	Lake shore	Loamy sand	49	31	20	8.35	23.12	1.57	4.34	1.30

2.6. Data Used

LD is influenced by a variety of factors [30], necessitating the use of diverse evaluation criteria, as outlined in Table 3. Data for this study were collected from multiple sources, including RS imagery such as Landsat-8, was downloaded from the United States Geological Survey website (https://earthexplorer.usgs.gov/, accessed on 27 April 2025), acquired on 6 January 2025, a Digital Elevation Model (DEM) with a 12.5 m resolution, derived from the Advanced Land Observing Satellite (ALOS-PALSAR), obtained from Alaska Satellite Facility (ASF) portal (https://www.asf.alaska.edu/sar-data/palsar/, accessed on 27 April 2025). Additional data were collected through field observations, laboratory analyses, and climatic conditions. The imagery was processed and analyzed using ENVI 5.3 software, which included steps such as atmospheric correction (using the FLAASH module), and spatial subsets. Following this, ISO DATA unsupervised classification was performed, succeeded by a maximum likelihood supervised classification. The Normalized Difference Vegetation Index (NDVI) was computed using the following Equation (1):

$$\mathrm{NDVI} = \frac{\mathrm{NIR} - \mathrm{Red}}{\mathrm{NIR} + \mathrm{Red}} \quad (1)$$

where NIR is Landsat-8 near-infrared band (band 5) and Red is Landsat-8 Red band (band 4).

Table 3. Land degradation data parameters.

Parameter	Class 1	Class 2	Class 3	Class 4	Class 5	Reference	Index
Parent Material	Shale, schist, basic, ultra-basic, conglomerates, unconsoli-dated	Limestone, marble, granite, rhyolite, ignimbrite, gneiss, siltstone, sandstone	Marl, Pyroclastic	-	-	[31]	Geology
Slope (%)	Gently sloping: <5	Sloping: 5–10	Strongly sloping: 10–15	Moderately steep: 15–30	Steep: 30–60	[32]	Topography
Aspect	North	South	Flat	East	West		
Topographic Wetness Index (TWI)	Very high: >5	High: 5–4	Moderate: 4–3	Low: 3–2	Very low: <2		
Curvature	Linear: −0.1 to 0.1	Convex: >0.1	Concave: <−0.1	-	-		
Depth (cm)	Very deep: >150	Deep: 150–100	Moderately deep: 100–50	Shallow: 50–30	Very shallow: <30	[28]	Physical Soil Quality
Gravel (%)	Few: <5	Common: 5–15	Many: 15–40	Abundant: 40–80	Dominant: >80		
Texture	Clay	Sandy clay, silty clay	Sandy clay loam, silty clay loam, clay loam	Sandy loam, loam, silt loam, silt	Sand, loamy sand		
Bulk Density (BD, Mg/m^3)	None: <1.2	Slight: 1.2–1.4	Moderate: 1.4–1.6	Strong: 1.6–1.8	Extreme: >1.8		
pH	Neutral: 6.6–7.3	Slightly alkaline: 7.4–7.8	Moderately alkaline: 7.9–8.4	Strongly alkaline: 8.5–9.0	Very strongly alkaline: >9.0	[33]	Chemical Soil Quality
Electrical Conductivity (EC, dS/m)	None: <4	Slight: 4–8	Moderate: 8–16	Strong: 16–32	Extreme: >32		
Exchangeable Sodium Percentage (ESP)	None: <10	Slight: 10–15	Moderate: 15–30	Strong: 30–50	Extreme: >50		
Organic Matter (OM, g/kg)	Very high: >50	High: 50–30	Moderate: 30–17	Low: 17–10	Very low: <10		
$CaCO_3$ (g/kg)	Non-calcareous: 0	Slightly calcareous: 0–20	Moderately calcareous: 20–100	Strongly calcareous: 100–250	Extremely calcareous: >250		
Gypsum (g/kg)	Non-gypsiferous: 0	Slightly gypsiferous: 0–50	Moderately gypsiferous: 50–150	Strongly gypsiferous: 150–600	Extremely gypsiferous: >600		

Table 3. *Cont.*

Parameter	Class 1	Class 2	Class 3	Class 4	Class 5	Reference	Index
Climate Erosivity Factor (CEF)	Very low: <20	Low: 20–50	Moderate: 50–70	Severe: 70–100	Extreme: >100	[34]	Wind Erosion
Soil Erodible Fraction (EFF, %)	Very slight: <0.2	Slight: 0.2–0.3	Moderate: 0.3–0.4	High: 0.4–0.5	Very high: >0.5		
Surface Crust Factor (SCF)	Very high: <0.1	High: 0.1–0.3	Moderate: 0.3–0.5	Low: 0.5–0.7	Very low: >0.7		
Surface Roughness Factor (SRF)	Very high: <0.15	High: 0.15–0.3	Moderate: 0.3–0.5	Low: 0.5–0.7	Very low: >0.7		
Vegetation Cover Factor (VCF)	Very high density: >0.8	High density: 0.8–0.6	Moderate density: 0.6–0.4	Low density: 0.4–0.2	Very low density: <0.2		
NDVI	Very high: >0.6	High: 0.6–0.5	Moderate: 0.5–0.4	Low: 0.4–0.3	Very low: <0.3	[35]	Vegetation

Additionally, ArcGIS 10.8 (ESRI Co, Redlands, CA, USA), slope classes, aspect, topographic wetness index (TWI), and curvature were extracted from the DEM. The TWI was calculated based on the method proposed by Haghighi et al., 2021 [36], using the following Equation (2):

$$\mathrm{TWI} = \mathrm{Ln}\left(\frac{\mathrm{A_s}}{\tan\beta}\right) \quad (2)$$

where A_s represents the flow accumulation raster local upslope and β is the slope raster values.

2.7. Modeling Land Degradation (LD)

The process of modeling LD involved four key steps. First, the criteria were selected, followed by assigning a rating for each criterion. Next, six indices were developed, focusing on topography, physical soil properties, chemical soil properties, wind erosion, and vegetation. Finally, the final LD map was generated. Using GIS tools, a thematic map layer was created for each criterion, and each layer was assigned a score ranging from 0.1 to 1.0, as shown in Table 3. In this scoring system, 0.1 represented the lowest class (least severe) for the specific LD index, while 1.0 represented the highest class (most severe or triggering).

Six indices were developed to characterize LD: the Geology Index (GI), Topographic Quality Index (TQI), Physical Soil Quality Index (PSQI), Chemical Soil Quality Index (CSQI), Wind Erosion Quality Index (WEQI), and Vegetation Quality Index (VQI), and the final LD index was calculated using the following Equation (3).

$$\mathrm{LD} = f(\mathrm{GI}, \mathrm{TQI}, \mathrm{PSQI}, \mathrm{CSQI}, \mathrm{WEQI}, \mathrm{VQI}) \quad (3)$$

In this study, the equal LD indices weights were assigned based on; sensitivity analyses showing comparable predictive power across indices (±15% output variation), and alignment with established frameworks like MEDALUS (Kosmas et al., 1999) [31]. The natural breaks method of ArcGIS 10.8 was used to divide the LD intensity into the following five classes, which minimizes within class variance while maximizing between class differences [30,37,38], as detailed in Table 4:

Table 4. Land degradation index classes and rates.

	Class	Rate
Land degradation	Very low	<0.2
	Low	0.2–0.4
	Moderate	0.4–0.6
	High	0.6–0.8
	Very high	>0.8

2.7.1. Wind Erosion Quality Index (WEQI): The Index of Land Susceptibility to Wind Erosion (ILSWE)

The WEQI was calculated based on the ILSWE index that is a quantitative measure used to assess the severity of wind erosion in a given area, developed by Fenta et al., 2020 [34], the ILSWE integrates multiple factors that influence wind erosion, providing a comprehensive evaluation of land vulnerability. The index is calculated using the Climatic Erosive Factor (CEF), Wind-Erodible Fraction Factor (EFF), Soil Crust Factor (SCF), Vegetation Cover Factor (VCF), and Surface Roughness Factor (SRF), as in the following Equation (4):

$$\text{ILSWE} = f(CEF,\ EFF,\ SCF,\ VCF,\ SRF) \quad (4)$$

The Climatic Erosive Factor (CEF)

The CEF is a key component in calculating the ILSWE index, and it quantifies the influence of climatic conditions on the potential for wind erosion in a specific area. The CEF is calculated using mean monthly wind speed, potential evapotranspiration, and monthly precipitation [34], as shown in Equation (5):

$$\text{CEF} = \frac{1}{100}\sum_{i=1}^{i=12} W_i^3 \left[\frac{\text{PET}_i - \text{P}_i}{\text{PET}_i}\right] \times d_i \quad (5)$$

where W_i is the mean monthly wind speed (m s^{-1}) at 2 m height in month i, PET_i is the potential evapotranspiration (mm) in month i, P_i is the precipitation (mm) in a month i, and d_i is the total number of days in the month i.

Wind-Erodible Fraction Factor (EFF)

EFF is a key parameter used in wind erosion models, such as the Wind Erosion Prediction System (WEPS) and the Revised Wind Erosion Equation (RWEQ), to estimate the susceptibility of soil to erosion by wind. It quantifies the proportion of soil aggregates that are small enough (typically < 0.84 mm in diameter) to be easily transported by wind.

EFF is typically expressed as a percentage or decimal fraction (0 to 1) [39]. The EF is calculated using the following Equation (6):

$$\text{EFF} = \frac{29.09 + 0.31\text{SA} + 0.17\text{SI} + 0.33\frac{\text{SA}}{\text{CL}} - 2.59\text{SOM} - 0.95\text{CaCO}_3}{100} \quad (6)$$

where EFF is expressed in percent, SA is the sand content, SI is the silt content, CL is the clay content, OM is the organic matter content.

The EFF is adjusted for clay content, organic matter, and surface crusting. Higher sand and silt contents generally increase the EFF, as these particles are more easily transported by wind. In contrast, higher clay content, organic matter, and calcium carbonate tend to reduce the EFF, as they improve soil stability and resistance to erosion. By quantifying these factors, the EFF provides a critical input for assessing wind erosion risk in the ILSWE index.

Soil Crust Factor (SCF)

The SCF is a parameter used in wind erosion models to account for the inhibitory effect of surface crusting on wind-driven soil erosion. Soil crusts formed by rainfall, biological activity, or salt cementation reduce erosion by increasing surface stability and cohesion. In this study, the SCF was estimated based on soil properties (e.g., clay content (CL), organic matter (OM)) and recent rainfall data, following the approach of Fenta et al., 2020 [34] as represented in Equation (7):

$$SCF = \frac{1}{1 + 0:0066(CL)^2 + 0.21(OM)^2} \quad (7)$$

The SCF quantifies how much a soil crust reduces wind erodibility compared to bare, loose soil. The SCF is expressed as a dimensionless factor (0 to 1), where SCF = 1: No crust (fully erodible) and SCF = 0: Complete crust (no erosion possible) [40].

Vegetation Cover Factor (VCF)

The VCF is a critical parameter in soil erosion models (both wind and water erosion) that quantifies how effectively plant cover protects the soil from erosion. It is expressed as a dimensionless ratio (0 to 1), where VCF = 0: Dense vegetation (maximum protection, negligible erosion), and VCF = 1: Bare soil (no protection, highest erosion risk). The VCF is computed using the following Equation (8) [41]:

$$VCF = 1 - \frac{NDVI - NDVI_{min}}{NDVI_{max} - NDVI_{min}} \quad (8)$$

The VCF captures the protective effect of vegetation in stabilizing the soil surface and minimizing wind erosion. This factor is essential for accurately assessing land susceptibility to wind erosion and guiding land management practices aimed at reducing erosion risks.

Surface Roughness Factor (SRF)

The SRF is a critical parameter in soil erosion models that quantifies how soil surface irregularities (clods, ridges, vegetation residues) reduce erosion by disrupting wind flow and rougher surfaces trap soil particles and lower wind speed near the ground [42].

SRF is a dimensionless index (0 to 1) where SRF = 0: Perfectly smooth surface (max erosion risk), and SRF > 1: very rough surfaces (e.g., deep tillage ridges) that significantly reduce erosion. The SRF is computed using the following Equation (9):

$$SRF = \frac{DEM_{mean} - DEM_{min}}{DEM_{max} - DEM_{min}} \quad (9)$$

In this equation, DEM_{mean} is the mean elevation value within the analysis area, DEM_{min} is the minimum elevation value within the analysis area, and DEM_{max} is the maximum elevation value within the analysis area.

The calculation of SRF is performed using focal statistics tools within ArcGIS 10.8, which analyze elevation data from a Digital Elevation Model (DEM). By quantifying surface roughness, the SRF provides valuable insights into how land surface characteristics influence wind erosion, aiding in the development of effective land management and erosion control strategies [43].

2.8. Geostatistical Analysis

Geostatistical analysis was conducted using the geostatistical analyst tools ArcGIS tools to predict and map soil attributes in unsampled areas. The Ordinary Kriging (OK) method, recognized as one of the most robust and widely used interpolation

techniques [44,45], was employed for this purpose. The OK method estimates the value of an unsampled value Z (S_0), as a linear combination of neighboring observed values, as expressed by the following Equation (10):

$$Z(S_0) = \sum_{i=1}^{N} \lambda_i \times Z(S_i) \quad (10)$$

where λ_i represents the unknown weight assigned to the measured value at the ith location, $Z(S_i)$ is the measured value at the ith location, and N is the total number of measured values used in the interpolation. The OK method utilizes various prediction models to optimize the interpolation process. Among these, the spherical, exponential, and Gaussian models are the most widely accepted and commonly used as the optimal semi-variogram based on lowest RMS error (0.024) during cross-validation [45,46], a variable search radius was used with a minimum of 5 and maximum of 15 neighboring points, a lag size of 2500 m was applied to match the average sampling density, and anisotropy was accounted for using a 45° azimuth with 1.5 ratio to address observed spatial autocorrelation patterns. These models help to accurately predict soil attributes across unsampled areas, providing valuable insights for spatial analysis and decision-making in land management.

2.9. Model Validation

The performance of the geostatistical models (Ordinary Kriging (OK)) used for predicting soil properties was evaluated using the cross-validation technique [47], a widely accepted method for assessing the accuracy and reliability of interpolation models. Such a verification considered prediction errors, including the Mean Error (ME), which measures the average difference between predicted and observed values to indicate bias; the Root Mean Square Error (RMSE), which quantifies the average magnitude of prediction errors to assess overall accuracy; the Mean Standardized Error (MSE), which evaluates the consistency of errors by assessing the average standardized difference between predicted and observed values; the Root Mean Square Standardized Error (RMSSE), which examines the variability of standardized errors to determine the reliability of the model's error estimates; and the Average Standardized Error (ASE), which provides insight into the model's precision by representing the average of standardized errors [48].

3. Results

3.1. Geology Index (GI)

The Damietta Governorate, as illustrated in Figure 5, is predominantly characterized by varying types of geological formations, each contributing differently to the overall composition of the region. The most significant formation is Nile silt, which spans 731.11 km^2, accounting for 69.91% of the total area. This type of land cover is considered to be of high-quality parent material, making it the dominant and most valuable component of the study area.

The second most prominent geological formation is stabilized sand dunes, covering 77.05 km^2 and representing 12.99% of the study area. These stabilized dunes are followed by sand dunes, which cover 60.32 km^2 and account for 11.26% of the area. Both types of sand dunes are classified as moderate-quality parent materials. While they may not be as fertile or nutrient-rich as Nile silt, they still provide a stable foundation for certain types of vegetation and land use, particularly in arid or semi-arid environments where stabilization is crucial for preventing desertification.

Additionally, undifferentiated quaternary deposits cover 39.79 km^2, making up 5.13% of the study area. These deposits are also categorized as moderate quality parent materials. Quaternary deposits typically consist of sediments that have been transported and

deposited by various geological processes, such as wind, water, or ice. While they may not be as fertile as Nile silt, they still offer a reasonable level of soil quality for certain types of land use.

The least significant land cover type in the study area is sabkha deposits, which cover only 2.83 km^2 and represent a mere 0.71% of the total area. Sabkha formations are classified as low-quality parent materials due to their high salinity and poor drainage, which make them unsuitable for most agricultural or developmental activities.

3.2. Topographic Quality Index (TQI)

The spatial distribution of TQI, as illustrated in Figure 8, is determined by analyzing key topographic factors, including slope, aspect, Topographic Wetness Index (TWI), and curvature. These factors collectively provide a comprehensive understanding of the terrain's characteristics and their influence on land quality within the study area.

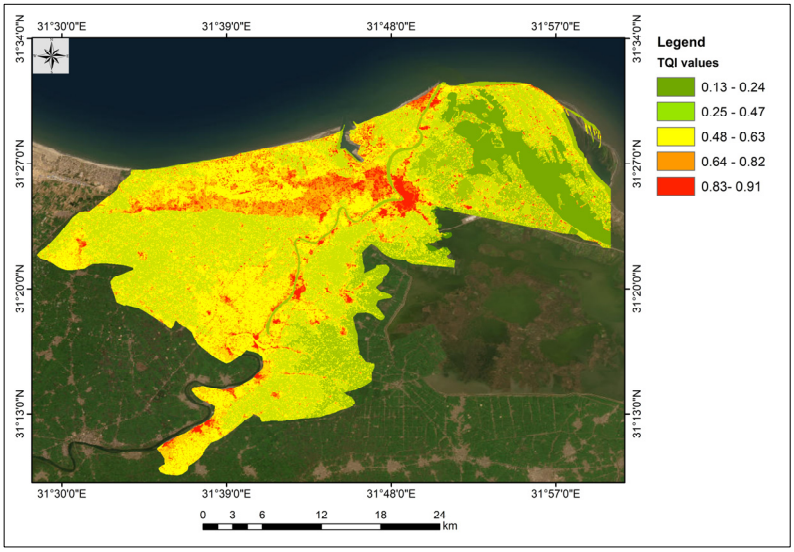

Figure 8. Topographic Quality Index (TQI) values in the investigated area.

The slope gradient, derived from a Digital Elevation Model (DEM), ranges from 0% to 69%, reflecting a transition from flat to very steep slopes, based on FAO, 2006 classification [28]. This wide range of slopes highlights the region's topographic diversity, with flat areas suitable for agriculture and construction, while steep slopes may present challenges such as erosion and instability, limiting their usability.

The aspect map reveals that slopes facing south, north, northeast, and northwest dominate the study area. Aspect plays a critical role in determining sunlight exposure, moisture retention, and vegetation growth. For instance, south-facing slopes typically receive more sunlight, which can increase soil temperature and evaporation rates, while north-facing slopes may retain more moisture, influencing soil fertility and land use suitability.

The TWI, which ranges from 2.46 to 13.71, indicates a gradient from moderate to very high wetness degrees [49]. TWI measures the potential for water accumulation in an area, with higher values suggesting greater soil moisture and potential for waterlogging.

The topographic curvature map shows values ranging from −6.38 to 7.29, with convex and concave surfaces dominating the study area, while flat surfaces cover only small portions. Curvature influences water flow and erosion patterns, with convex areas promoting runoff and concave areas facilitating water accumulation.

The TQI values range from 0.13 to 0.91, reflecting a spectrum of land quality from very high to very low. The spatial distribution of these quality grades, as detailed in Table 5, shows that very high-quality areas cover 3.16% of the total study area, and these

regions are characterized by favorable topographic conditions, such as moderate slopes, optimal aspect, and balanced wetness. High-quality areas cover 3.86% of the study area, exhibiting slightly less optimal but still favorable conditions. Moderate-quality areas dominate the study area, covering 47.82%, and while they may have some limitations, such as steeper slopes or less ideal wetness conditions, they remain suitable for a range of land uses with proper management. Low-quality areas make up 41.37% of the study area, constrained by factors such as steep slopes, poor drainage, or unfavorable aspect, limiting their suitability for intensive land use. Finally, very low-quality areas cover 3.79% of the total area, characterized by extreme topographic conditions, such as very steep slopes or excessive wetness, rendering them unsuitable for most agricultural or developmental activities.

Table 5. Spatial distribution of LD classes and its areas in the investigated area.

Land Degradation Index	Quality Class	Area %	Spatial Distribution
Topographic Quality Index (TQI)	Very high	3.16%	
	High	3.86%	
	Moderate	47.82%	
	Low	41.37%	
	Very low	3.79%	
Physical Quality Index (PQI)	Very high	0.00%	
	High	14.03%	
	Moderate	68.14%	
	Low	17.83%	
	Very low	0.00%	
Chemical Quality Index (CQI)	Very high	4.05%	
	High	33.70%	
	Moderate	51.54%	
	Low	10.71%	
	Very low	0.00%	
Wind Erosion Quality Index (WEQI)	Very high	0.00%	
	High	27.41%	
	Moderate	65.73%	
	Low	6.86%	
	Very low	0.00%	
Vegetation Quality Index (VQI)	Very high	31.41%	
	High	21.54%	
	Moderate	20.67%	
	Low	15.59%	
	Very low	10.79%	

3.3. Physical Quality Index (PQI)

The spatial distribution of PQI attributes, including effective depth, gravel content, texture, and bulk density (BD) is depicted in Figure 9. The results reveal significant variability in soil characteristics across the study area. Soil depth ranges from 100 to 150 cm, indicating a deep soil profile. Gravel content varies from 2.1% to 18.7%, classified as few to many gravel contents according to [28]. While moderate gravel content can improve soil drainage and aeration, higher gravel content may reduce water and nutrient retention, potentially limiting soil productivity in certain areas.

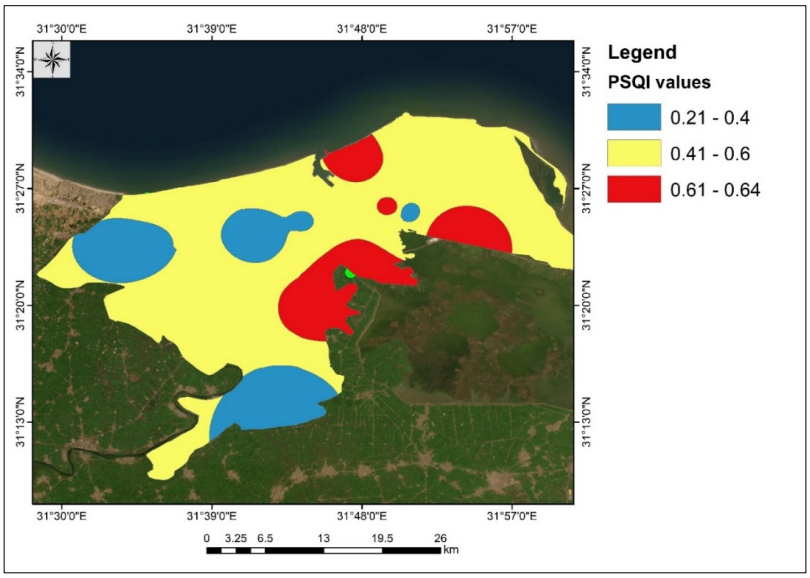

Figure 9. Physical Quality Index (PQI) values in the investigated area.

The soil texture analysis shows that sand dominates the particle size distribution, ranging from 32.6% to 57.3% and averaging 53.6% of the fine earth fraction, this is followed by silt (14.7% to 29.4%, averaging 24.1%) and clay (8.6% to 25.13%, averaging 22.3%). The predominance of sand suggests that the soils are generally well-drained but may have lower water and nutrient-holding capacities compared to soils with higher silt or clay content.

The bulk density (BD) of the soils ranges from 2.1 to 2.8 mg m^{-3}, indicating moderate to strong compaction hazards according to [50]. Higher bulk density values suggest that the soils are compacted, which can restrict root penetration, reduce water infiltration, and limit aeration, thereby negatively impacting plant growth and soil quality. Areas with lower bulk density are more favorable for agricultural activities, as they allow for better root development and water movement.

The PQI analysis, as presented in Table 5, categorizes the soils into three quality degrees based on their physical attributes. Soils with low physical quality cover 17.83% of the study area, likely characterized by high gravel content, poor texture, or high bulk density, which limit their suitability for intensive land use. Moderate-quality soils dominate the area, covering 68.14% of the studied area, indicating that while these soils may have some limitations, they are generally suitable for a range of agricultural and developmental activities with proper management. High-quality soils, which occupy 14.03% of the total area, are characterized by favorable physical attributes such as deep soil profiles, balanced texture, and low bulk density that meet FAO criteria for intensive agriculture.

3.4. Chemical Quality Index (CQI)

The spatial distribution of chemical soil quality attributes, including pH, electrical conductivity (EC), exchangeable sodium percentage (ESP), organic matter (OM), calcium

carbonate ($CaCO_3$), and gypsum content, is illustrated in Figure 10. The soil pH ranges from 7.3 to 8.5, indicating that the soils are slightly to strongly alkaline. The EC values range from 1.9 to 13.9 dS m^{-1}, classifying the soils as non-saline to strongly saline [51]. The ESP values vary from 6.4 to 13.7, indicating none to strong sodicity (alkalinity) hazards [50]. Soils with high ESP are prone to poor structural stability, reduced water infiltration, and surface crusting, which can hinder agricultural productivity. The organic matter (OM) content is low, ranging from 2.0 to 9.1 g kg^{-1}, which is insufficient to support robust soil fertility and microbial activity. Low OM levels can lead to poor soil structure, reduced water-holding capacity, and limited nutrient cycling. The calcium carbonate ($CaCO_3$) content ranges from 4.2 to 94.6 g kg^{-1}, indicating that the soils are moderate to extremely calcareous [28]. High $CaCO_3$ content can influence soil pH and nutrient availability, particularly phosphorus, which tends to become less available in calcareous soils. The gypsum content varies from 1.6 to 29.7 g kg^{-1}, classifying the soils as slightly gypsiferous. While moderate gypsum content can improve soil structure and reduce sodicity, excessive amounts may lead to soil dispersion and reduced stability.

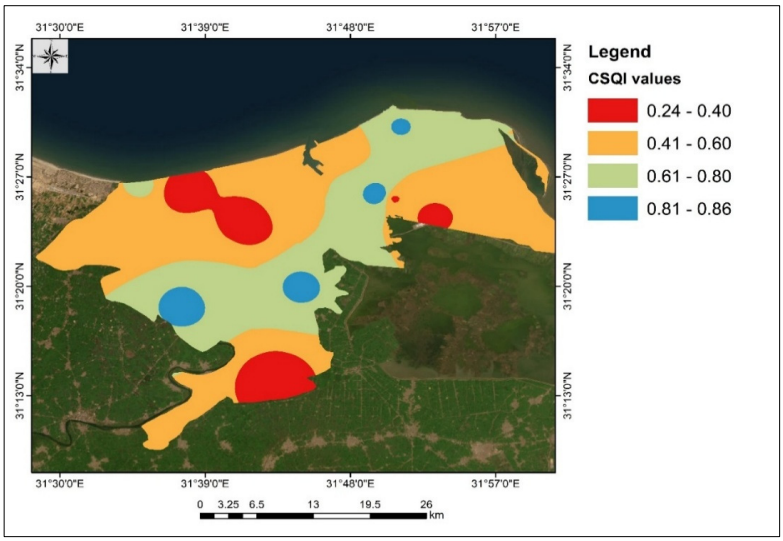

Figure 10. Chemical Quality Index (CQI) values in the investigated area.

The spatial analysis, as summarized in Table 5, reveals that low chemical quality soils cover 10.71% of the study area. These soils are characterized by high salinity, sodicity, or low OM content, making them less suitable for productive land use without significant remediation. Moderate-quality soils dominate the area, covering 51.54% of the studied area, indicating that while these soils may have some chemical limitations. High and very high-quality soils cover 33.70% and 4.05% of the total study area, respectively. These soils exhibit favorable chemical properties, such as balanced pH, low salinity, and adequate OM content.

3.5. Wind Erosion Quality Index (WEQI): The Index of Land Susceptibility to Wind Erosion (ILSWE)

The spatial distribution of the wind erosion hazards parameters including climate erosivity (CEF), soil erodibility (EFF), soil crust (SCF), surface roughness (SRF), and vegetation cover (VCF) is illustrated in Figure 11.

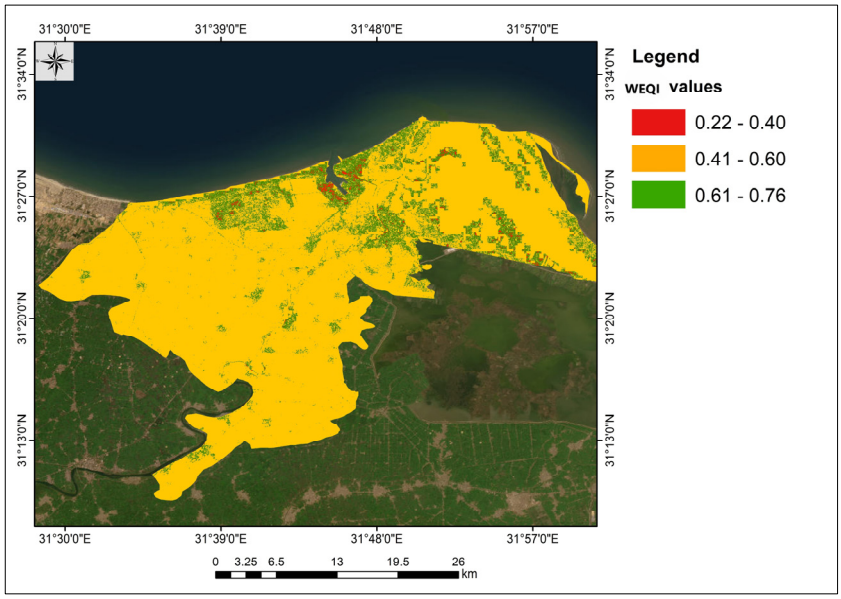

Figure 11. Wind Erosion Quality Index (WEQI) values in the investigated area.

The study area is characterized by a moderate climate hazard, with a CEF value of 62.74, corresponding to a score of 0.6 [52]. This indicates that the region experiences moderate wind-driven erosive forces, which can contribute to soil degradation if not managed properly. The EFF values range from 0.36 to 0.58, reflecting moderate to very high soil erodibility [53]. Soils with higher erodibility are more susceptible to wind erosion, particularly in areas with limited vegetation cover or poor soil structure.

The soil crust factor (SCF) varies from 0.18 to 0.84, indicating a gradient from high to very low surface crust [52]. Surface crusting can reduce soil erodibility by protecting the soil surface, but areas with low SCF values are more vulnerable to wind erosion due to the lack of a protective crust. The surface roughness factor (SRF) ranges from 0.13 to 0.82, representing very high to very low surface roughness [54]. Rough surfaces, such as those with vegetation residues or microtopographic variations, can reduce wind erosion by disrupting airflow and trapping soil particles, while smoother surfaces are more prone to erosion.

The vegetation cover factor (VCF) varies from 0 to 1, indicating very low to very high vegetation density [55]. Vegetation plays a critical role in mitigating wind erosion by stabilizing the soil surface, reducing wind speed at ground level, and trapping airborne particles.

The spatial analysis, as summarized in Table 5, reveals that 27.41% of the total area is under high erosion risk, primarily due to factors such as high soil erodibility, low surface crust, low surface roughness, and sparse vegetation cover. The majority of the study area (65.73%) falls under moderate erosion risk, indicating that while these regions are susceptible to erosion, the risk is manageable with appropriate land management practices, such as conservation tillage, cover cropping, or improved vegetation cover. Only 6.86% of the area is classified as having low erosion risk, likely due to favorable conditions such as high vegetation density, rough surfaces, or protective soil crusts.

3.6. Vegetation Quality Index (VQI)

The VQI, derived from the NDVI, ranges from 0.058 to 0.57, reflecting a gradient from very high to very low vegetation quality, as shown in Table 5 [56]. As shown in Figure 12, the spatial distribution of VQI reveals that very high vegetation quality is the predominant class in the study area, covering 31.41% of the total area, and these regions are characterized by dense and healthy vegetation, which plays a vital role in preventing soil erosion, enhancing

water retention, and supporting biodiversity. Areas with high vegetation quality covered 21.54% of the study area, while slightly less dense than very high-quality areas, these regions still support robust vegetation cover, contributing to ecosystem services such as carbon sequestration and habitat provision. Moderate vegetation quality areas covered 2067% of the total area, indicating regions with intermediate vegetation density and quality, these areas may require targeted management practices, such as reforestation or sustainable grazing, to improve vegetation quality and prevent degradation. In contrast, low vegetation quality areas cover 15.56% of the study area, representing regions with sparse or stressed vegetation, and these areas are more vulnerable to environmental challenges such as soil erosion, desertification, and reduced agricultural productivity. Finally, very low vegetation quality areas cover 10.79% of the total area, indicating regions with minimal or degraded vegetation cover, these areas are characterized by harsh environmental conditions, such as poor soil quality, limited water availability, or human-induced LD, and require significant restoration efforts to improve vegetation quality and ecosystem functionality.

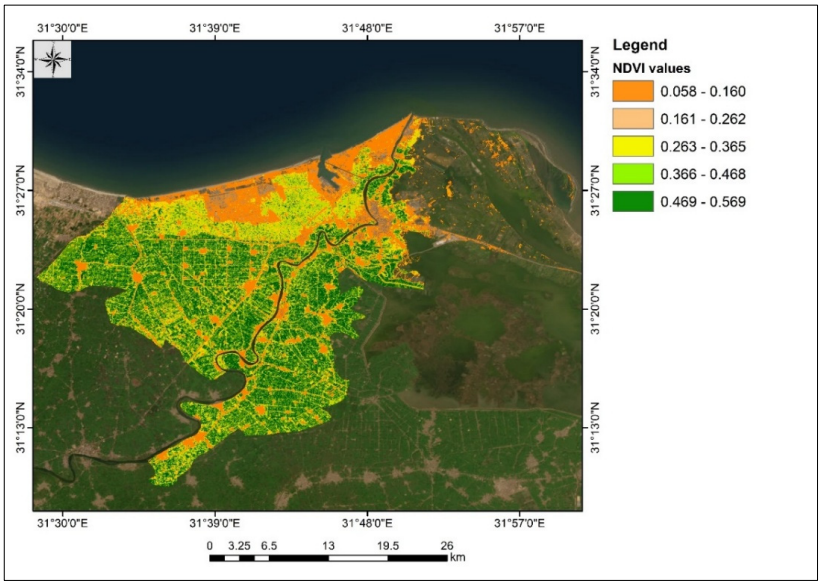

Figure 12. Vegetation Quality Index (VQI) values in the investigated area.

3.7. The Spatial Distribution of Land Degradation (LD) Hazards

The land degradation (LD) map, as shown in Figure 13, reveals that the values of LD range from 0.27 to 0.84, indicating a gradient from low to very high degradation hazards. This variability reflects the diverse environmental and anthropogenic pressures affecting the study area. The spatial distribution of LD, shows that the study area is vulnerable to varying degrees of degradation. Low degradation hazards cover 32.70% of the total area, representing regions with relatively stable and healthy ecosystems that are less affected by degradation processes; these areas are characterized by good soil quality, adequate vegetation cover, and sustainable land management practices. Moderate degradation hazards affect 35.48% of the study area, indicating regions where degradation processes, such as soil erosion, vegetation loss, or declining soil fertility, are beginning to take hold but are not yet severe. High degradation hazards impact 17.39% of the total area, representing regions where degradation is more advanced; with significant impacts on soil productivity, vegetation cover, and ecosystem services, these areas are at greater risk of desertification, reduced agricultural yields, and biodiversity loss, necessitating urgent and targeted interventions to mitigate degradation and restore land functionality. A smaller but significant portion of the study area (14.44%) is classified as having very high degradation hazards, indicating regions where degradation processes are severe and

potentially irreversible without extensive restoration efforts, these areas are characterized by extreme soil erosion, barren landscapes, and minimal vegetation cover.

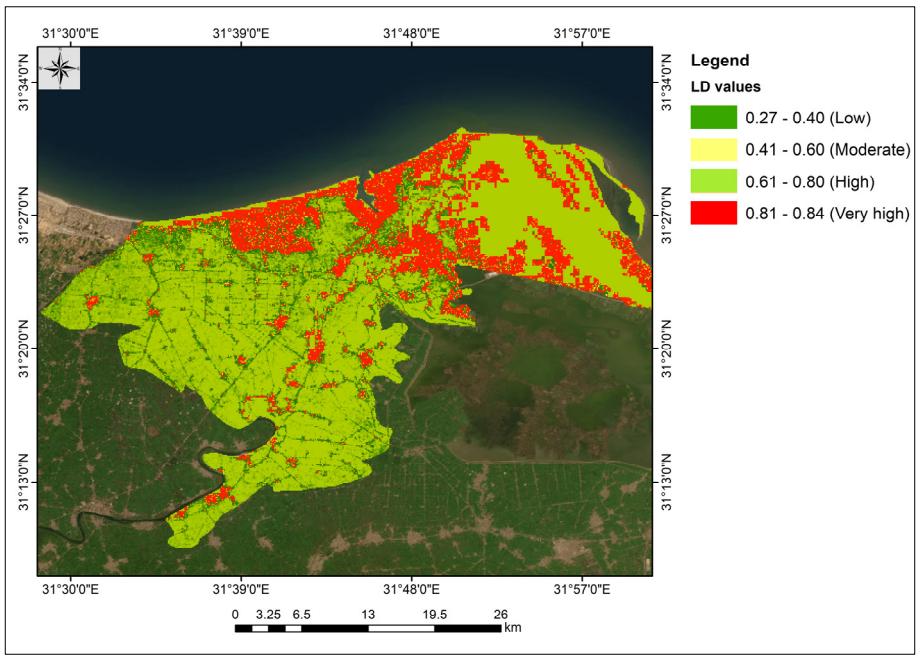

Figure 13. Land degradation map in the studied area.

3.8. Land Degradation (LD) Map Validation

The cross-validation results, as presented in Table 6, demonstrate the accuracy and reliability of the OK models used for predicting soil properties. The ME and MSE values were found to be close to 0, indicating that the models produced unbiased predictions with minimal systematic errors. Additionally, the RMSSE values were close to 1.0, suggesting that the prediction errors were well-calibrated and consistent with the model's assumptions. However, the RMSE and ASE values, while similar to each other, were relatively higher for most of the studied soil properties. This indicates that, although the models performed well in terms of bias and calibration, there was still a degree of variability in prediction accuracy across different properties.

Table 6. Evaluation of prediction accuracy: cross-validation of Ordinary Kriging models.

Metric	Depth	Gravel	Bulk Density (g/cm^3)	Sand	Silt	Clay	EC (ds/m)	ESP	$CaCO_3$ (%)	Gypsum	pH	OM	EF	SCF
Model	Expo.	Sph.	Sph.	Sph.	Expo.	Sph.	Gaus.	Gaus.	Expo.	Expo.	Expo.	Sph.	Expo.	Sph.
ME	−0.022	0.146	−0.003	−0.019	0.040	0.082	−0.117	0.117	0.128	0.062	−0.005	−0.011	0.006	−0.008
RMSE	15.364	6.778	0.119	12.650	8.505	6.751	14.792	6.880	18.104	11.401	0.404	2.325	0.091	0.026
MSE	0.004	−0.071	−0.037	−0.014	−0.062	−0.125	−0.009	0.030	−0.053	−0.037	−0.034	−0.016	0.069	−0.142
RMSSE	1.391	1.308	1.410	1.270	1.378	1.466	1.316	1.431	1.554	1.447	1.430	1.364	1.246	1.260
ASE	15.211	8.688	0.117	13.631	8.378	6.980	15.415	6.556	19.706	10.507	0.386	2.291	0.098	0.315

Expo. = Exponential, Sph. = Spherical, Gaus. = Gaussian.

The results also highlight the suitability of different variogram models for predicting specific soil properties. The Exponential model was found to be the most appropriate for six soil properties: soil depth, calcium carbonate ($CaCO_3$) content, gypsum content, erodibility factor (EF), silt content, and pH. This suggests that these properties exhibit spatial patterns best described by an exponential decay in spatial autocorrelation. The Spherical model was suitable for another six properties: gravel content, bulk density, soil crust factor (SCF), sand content, clay content, and organic matter (OM), and this indicates that these properties follow a spatial structure where autocorrelation decreases linearly up to a certain distance

before leveling off. Finally, the Gaussian model was found to be appropriate for only three properties: electrical conductivity (EC) and exchangeable sodium percentage (ESP), this implies that these properties exhibit a smoother, more gradual spatial variation.

4. Discussion

4.1. The Geological Index

The GI in Damietta Governorate reveals a landscape dominated by Nile silt (69.91%), which is consistent with other studies in the Nile Delta that highlight its critical role in supporting agriculture due to its high fertility and nutrient content [57]. Similar patterns are observed globally in other riverine systems, such as the Ganges-Brahmaputra and Mississippi Deltas, where alluvial soils are vital for food production [58]. The presence of stabilized sand dunes (12.99%) and sand dunes (11.26%) reflects the region's semi-arid conditions, aligning with studies in Egypt's Western Desert and Sinai Peninsula [59], as well as the Central Loess Plateau, where dune stabilization is essential for combating desertification [60]. The undifferentiated quaternary deposits (5.13%) and sabkha formations (0.71%) further emphasize the region's geological diversity, mirroring findings in other deltaic and arid coastal areas worldwide, such as the Mekong Delta [61] and Arabian Peninsula [62], where similar deposits influence land use potential.

4.2. Topographic Quality Index

The results of TQI in Damietta Governorate align with both local and global research on the influence of topographic factors on land quality [63]. The dominance of moderate-quality areas (47.82%) and the significant presence of low-quality areas (41.37%) reflect the region's diverse topography, characterized by varying slopes, aspects, and wetness conditions. Similar patterns have been observed in other parts of the Nile Delta, where flat to gently sloping terrains support agriculture, while steeper slopes and areas with high wetness pose challenges for land use. Globally, studies in regions such as Mississippi River Basin have also highlighted the critical role of slope, aspect, and wetness in determining land suitability, emphasizing the universal importance of these factors in land quality assessment [64]. The limited extent of very high-quality (3.16%) and high-quality (3.86%) areas underscores the need for targeted land management strategies to optimize the use of these fertile zones. This finding is consistent with research in other deltaic and coastal regions, where high-quality land is often scarce and requires careful conservation [65].

4.3. Physical Quality Index

The dominance of physical moderate-quality soils (68.14%) suggests that the majority of the study area is suitable for a range of agricultural and developmental activities, this result aligns with other studies in the Nile Delta [66], where moderate-quality soils have been shown to support sustainable agriculture. Globally, similar findings have been reported in regions such as the Indo-Gangetic Plain [67], and the Midwest United States [68], where moderate-quality soils form the backbone of agricultural systems, requiring careful management to maintain productivity. The presence of high-quality soils (14.03%), characterized by deep soil profiles, balanced texture, and low bulk density, highlights the suitability for intensive cropping systems in certain parts of Damietta Governorate, these areas are comparable to fertile regions, such as South America [69], where similar soil properties support intensive farming. Conversely, the low-quality soils (17.83%), with high gravel content, poor texture, or compaction issues, pose challenges for land use, similar conditions found in semi-arid and sub-tropical of India [70].

4.4. Chemical Quality Index

The chemical soil quality attributes reveal a landscape with varying degrees of soil fertility and suitability for agricultural and developmental activities [71]. The dominance of moderate-quality soils (51.54%) suggests that a significant portion of the study area can support productive land use with proper management practices to address limitations such as salinity, sodicity, and low organic matter content. This aligns with other studies in the Nile Delta, where moderate-quality soils have been shown to benefit from amendments such as gypsum, organic fertilizers, and improved irrigation techniques to enhance productivity [72]. The presence of high and very high-quality soils (37.75%), characterized by balanced pH, low salinity, and adequate organic matter, highlights the suitability for intensive cropping systems in certain areas, similar to fertile regions in the Mediterranean basin [73]. However, the low-quality soils (10.71%), with high salinity, sodicity, or low organic matter, pose significant challenges.

4.5. Wind Erosion Quality Index

The spatial distribution of wind erosion hazard parameters, including CEF, EFF, SCF, SRF, and VCF, reveals that the study area is predominantly characterized by moderate climate erosivity (CEF = 62.74) and moderate to very high soil erodibility (EFF = 0.36–0.58), consistent with findings by Richardson and Sadler, 2022 [52] and Abd-Elazem et al., 2024 [53]. The variability in SCF (0.18–0.84) and SRF (0.13–0.82) highlights the importance of surface crusting and roughness in mitigating erosion, as noted by Masri et al., 2015 [54], with low values increasing vulnerability to wind erosion. Vegetation cover (VCF = 0–1) plays a critical role in reducing erosion risk, aligning with study by Song et al., 2017 [55], who emphasized its stabilizing effect on soil surfaces. The spatial analysis indicates that 27.41% of the area is at high erosion risk due to factors such as high EFF, low SCF, and sparse VCF, while 65.73% is at moderate risk, similar to findings in other arid and semi-arid regions [52]. However, the proportion of low-risk areas (6.86%) is smaller compared to some studies by Gabriele et al., 2023 [74] and Sandeep et al., 2021 [30], suggesting that this region may require more targeted interventions.

4.6. Vegetation Quality Index

The VQI, highlights significant spatial variability in vegetation quality across the study area, with very high vegetation quality covering 21.41% of the region, consistent with findings by Shao et al., 2023 [56], who emphasized the critical role of dense and healthy vegetation in mitigating soil erosion and enhancing ecosystem services. High vegetation quality areas (11.54%) and moderate quality areas (15.59%) align with previous studies [52,55,63] that underscore the importance of intermediate vegetation density in supporting carbon sequestration and habitat provision, though these regions may require targeted interventions such as reforestation or sustainable grazing to prevent degradation, as noted in similar arid and semi-arid environments. In contrast, the substantial coverage of low (30.67%) and very low (20.79%) vegetation quality areas reflects heightened vulnerability to soil erosion, desertification, and reduced agricultural productivity, mirroring findings in regions with poor soil quality and limited water availability [35]. These areas necessitate extensive restoration efforts, as observed in other degraded landscapes, to improve vegetation quality and ecosystem functionality.

4.7. Land Degradation (LD) Mapping

The LD map, reveals a gradient from low to very high degradation hazards, reflecting the diverse environmental and anthropogenic pressures in the study area. Low degradation areas (32.70%) align with findings by Abowaly et al., 2022 [20], where stable ecosystems

with good soil quality and vegetation cover are less prone to degradation. Moderate degradation (35.48%) similar observations by Abdullahi et al., 2023 [14], highlighting regions where processes such as soil erosion and vegetation loss are emerging but not yet severe. High degradation (17.39%) and very high degradation (14.44%) areas, characterized by advanced soil erosion, reduced vegetation, and desertification risks, are consistent with studies in arid and semi-arid regions [13], emphasizing the need for urgent restoration efforts to mitigate irreversible damage. This is logic because scarce rainfall under semi-arid climate makes the modifications of major soil limitation (depth, salinity, and alkalinity) more difficult, and these findings underscore the importance of targeted land management strategies to address varying degradation levels and promote ecosystem resilience [17].

4.8. Map Validation

The study highlights the effectiveness of OK models in predicting soil properties, with ME and MSE values and RMSSE, indicating unbiased and well-calibrated predictions, consistent with study by Abuzaid et al., 2021 [35]. However, higher RMSE and ASE values reflect variability in accuracy, similar to findings by El Nahry et al., 2008 [19], emphasizing the challenges of extraction spatial heterogeneity. The suitability of the Exponential model for properties such as soil depth, $CaCO_3$, gypsum, EF, silt, and pH, the Spherical model for gravel, BD, SCF, sand, clay, and OM, and the Gaussian model for EC and ESP aligns with study by El-Gammal et al., 2015 [23], who stressed the importance of variogram model selection based on spatial patterns. These results reinforce the need for tailored modeling approaches to enhance prediction accuracy and inform sustainable land management practices [2].

5. Conclusions and Recommendations

This study provides a comprehensive assessment of land quality in Damietta Governorate, integrating geological, topographic, physical, chemical, wind erosion, vegetation, and LD indices. The findings reveal a landscape characterized by diverse soil and environmental conditions, with significant variability in land suitability for agriculture and development. The dominance of moderate-quality soils and areas with moderate degradation highlights the potential for sustainable land use, provided that appropriate management practices are implemented. However, the presence of low-quality soils, high erosion risks, and degraded areas underscores the need for targeted interventions to address challenges such as soil salinity, compaction, and vegetation loss. The validation of spatial models further emphasizes the importance of accurate data and tailored approaches for effective land management.

The GI analysis highlights the dominance of Nile silt, which is crucial for agriculture due to its high fertility and nutrient content. The presence of stabilized sand dunes and sand dunes reflects the region's semi-arid conditions, where dune stabilization is essential for combating desertification. The undifferentiated quaternary deposits and sabkha formations further emphasize the region's geological diversity.

The TQI results reveal that the region's diverse topography, characterized by varying slopes, aspects, and wetness conditions, significantly influences land quality. The dominance of moderate-quality areas and the significant presence of low-quality areas reflect the challenges posed by steep slopes and high wetness. The limited extent of very high-quality and high-quality areas underscores the need for targeted land management strategies to optimize the use of these fertile zones.

The PQI analysis indicates that the majority of the study area is covered by moderate-quality soils, which are suitable for a range of agricultural and developmental activities with proper management. The presence of high-quality soils, characterized by deep soil

profiles, balanced texture, and low bulk density, highlights the suitability for intensive cropping systems. Conversely, the low-quality soils, with high gravel content, poor texture, or compaction issues, pose challenges for land use.

The CQI analysis reveals a landscape with varying degrees of soil fertility, dominated by moderate-quality soils, which can support productive land use with proper management practices to address limitations such as salinity, sodicity, and low organic matter content. The presence of high and very high-quality soils, characterized by balanced pH, low salinity, and adequate organic matter, highlights suitability for intensive cropping systems. However, the low-quality soils, with high salinity, sodicity, or low organic matter, pose significant challenges.

The WEQI analysis indicates that the study area is predominantly characterized by moderate CEF and moderate to very high EFF. The variability in SCF and SRF highlights the importance of surface crusting and roughness in mitigating erosion, while VCF plays a critical role in reducing erosion risk. The spatial analysis indicates that 27.41% of the area is at high erosion risk, 65.73% is at moderate risk, and only 6.86% is at low risk, suggesting the need for targeted interventions to address wind erosion.

The VQI highlights significant spatial variability in vegetation quality, with very high vegetation quality covering. High vegetation quality areas and moderate quality areas underscore the importance of intermediate vegetation density in supporting carbon sequestration and habitat provision. In contrast, the substantial coverage of low and very low vegetation quality areas reflects heightened vulnerability to soil erosion, desertification, and reduced agricultural productivity.

The LD maps reveal a gradient from low to very high degradation hazards, reflecting the diverse environmental and anthropogenic pressures in the study area. Low degradation areas where stable ecosystems with good soil quality and vegetation cover are less prone to degradation. Moderate degradation highlights regions where processes such as soil erosion and vegetation loss are emerging but not yet severe. High degradation and very high degradation areas, characterized by advanced soil erosion, reduced vegetation, and desertification risks, emphasizing the need for urgent restoration efforts to mitigate irreversible damage.

Model validation represents the effectiveness of OK models in predicting soil properties, with ME and MSE values indicating unbiased and well-calibrated predictions. However, RMSE and ASE values reflect variability in accuracy, emphasizing the challenges of capturing spatial heterogeneity. The suitability of the Exponential model for properties such as soil depth, $CaCO_3$, gypsum, EFF, silt, and pH, the Spherical model for gravel, BD, SCF, sand, clay, and OM, and the Gaussian model for EC and ESP stress the importance of variogram model selection based on spatial patterns. These results reinforce the need for tailored modeling approaches to enhance prediction accuracy and inform sustainable land management practices. While the study demonstrates the effectiveness of OK models in predicting soil properties with unbiased and well-calibrated results (as indicated by ME, MSE, and RMSSE), this study acknowledges certain limitations, particularly its sensitivity to spatial heterogeneity. The higher RMSE and ASE values suggest variability in prediction accuracy, likely due to OK's assumption of stationarity, which may not fully capture abrupt changes or non-stationary trends in soil properties across complex landscapes. Additionally, while the tailored use of Exponential, Spherical, and Gaussian models improved interpolation for specific soil parameters, OK remains inherently limited by its reliance on spatial autocorrelation alone, without accounting for auxiliary variables or localized anomalies.

To address the challenges identified in Damietta Governorate, this study recommends the implementation of soil conservation practices, such as organic amendments and gypsum application, to improve soil fertility and structure, particularly in low-quality and

degraded areas. In addition, establishing monitoring systems using remote sensing to track degradation trends, and erosion control measures, including windbreaks and afforestation, should be prioritized in high-risk areas to mitigate wind erosion. Enhancing vegetation cover through reforestation and sustainable grazing practices can stabilize vulnerable ecosystems and improve soil quality and land use planning should focus on optimizing high-quality areas for intensive agriculture while rehabilitating degraded areas.

Author Contributions: Conceptualization, E.A.A., A.S.E., N.Y.R. and M.E.F.; methodology, E.A.A., A.S.E., N.Y.R. and M.E.F.; validation, E.A.A., A.S.E., N.Y.R. and M.E.F.; formal analysis, E.A.A., A.S.E., N.Y.R. and M.E.F.; investigation, E.A.A., A.S.E. and M.E.F.; resources, E.A.A., A.S.E., N.Y.R. and M.E.F.; data curation, E.A.A., A.S.E., N.Y.R. and M.E.F.; writing—original draft preparation, E.A.A., A.S.E. and M.E.F.; writing—review and editing, E.A.A., A.S.E., N.Y.R. and M.E.F.; visualization, E.A.A., A.S.E., N.Y.R. and M.E.F.; supervision, E.A.A. and M.E.F.; project administration, E.A.A., A.S.E., N.Y.R. and M.E.F.; funding acquisition, E.A.A., A.S.E., N.Y.R. and M.E.F. All authors have read and agreed to the published version of the manuscript.

Funding: This paper has been supported by the RUDN University Strategic Academic Leadership Program.

Institutional Review Board Statement: Not applicable.

Informed Consent Statement: Not applicable.

Data Availability Statement: Data are contained within the article.

Acknowledgments: The manuscript presented is a scientific collaboration between scientific institutions in two countries (Egypt and Russia). The authors would like to thank Zagazig University, National Authority for Remote Sensing and Space Science (NARSS), and RUDN University for support with the field survey, remote sensing and data analysis.

Conflicts of Interest: The authors declare no conflicts of interest.

References

1. Farooqi, Z.U.R.; Sohail, M.; Alserae, H.; Qadir, A.A.; Hussain, T.; Ilic, P.; Riaz, S.; Zafar, Z. Management of Soil Degradation: A Comprehensive Approach for Combating Soil Degradation, Food Insecurity, and Climate Change. In *Ecosystem Management: Climate Change and Sustainability*; Scrivener Publishing LLC.: Beverly, MA, USA, 2024; pp. 55–78.
2. El-Ramady, H.R.; El-Marsafawy, S.M.; Lewis, L.N. Sustainable agriculture and climate changes in Egypt. *Sustain. Agric. Rev.* **2013**, *12*, 41–95.
3. Gupta, G.S. Land degradation and challenges of food security. *Rev. Eur. Stud.* **2019**, *11*, 63. [CrossRef]
4. Schillaci, C.; Jones, A.; Vieira, D.; Munafò, M.; Montanarella, L. Evaluation of the United Nations Sustainable Development Goal 15.3. 1 indicator of land degradation in the European Union. *Land Degrad. Dev.* **2023**, *34*, 250–268. [CrossRef]
5. Sharma, S.; Beslity, J.O.; Rustad, L.; Shelby, L.J.; Manos, P.T.; Khanal, P.; Reinmann, A.B.; Khanal, C. Remote Sensing and GIS in Natural Resource Management: Comparing tools and emphasizing the importance of in-situ data. *Remote Sens.* **2024**, *16*, 4161. [CrossRef]
6. Prăvălie, R. Exploring the multiple land degradation pathways across the planet. *Earth-Sci. Rev.* **2021**, *220*, 103689. [CrossRef]
7. Kiprop, A.K. *Mapping Land Cover Changes and Identification of Drivers of Degradation to Inform Rehabilitation Strategies in Wenje, Tana River County*; University of Nairobi: Nairobi, Kenya, 2023.
8. Aboukota, M.E.S.; Hassaballa, H.; Elhini, M.; Ganzour, S.K. Land Degradation, Desertification & Environmental Sensitivity to Climate Change in Alexandria and Beheira, Egypt. *Egypt. J. Soil Sci.* **2024**, *64*, 167–180.
9. Selmy, S.A.; Kucher, D.E.; Moursy, A.R. Integrating Remote Sensing, GIS, and AI Technologies in Soil Erosion Studies. In *Advanced Geoinformatics—Techniques and Applications*; IntechOpen: London, UK, 2025. [CrossRef]
10. Karra, K.; Kontgis, C.; Statman-Weil, Z.; Mazzariello, J.C.; Mathis, M.; Brumby, S.P. Global land use/land cover with Sentinel 2 and deep learning. In Proceedings of the 2021 IEEE International Geoscience and Remote Sensing Symposium IGARSS, Brussels, Belgium, 11–16 July 2021; pp. 4704–4707.
11. Giuliani, G.; Mazzetti, P.; Santoro, M.; Nativi, S.; Van Bemmelen, J.; Colangeli, G.; Lehmann, A. Knowledge generation using satellite earth observations to support sustainable development goals (SDG): A use case on Land degradation. *Int. J. Appl. Earth Obs. Geoinf.* **2020**, *88*, 102068. [CrossRef]

12. Kawy, W.A.; Darwish, K.M. Assessment of land degradation and implications on agricultural land in Qalyubia Governorate, Egypt. *Bull. Natl. Res. Cent.* **2019**, *43*, 70. [CrossRef]
13. AbdelRahman, M.A.; Afifi, A.A.; Scopa, A. A time series investigation to assess climate change and anthropogenic impacts on quantitative land degradation in the North Delta, Egypt. *ISPRS Int. J. Geo-Inf.* **2022**, *11*, 30. [CrossRef]
14. Abdullahi, M.B.; Elnaggar, A.A.; Omar, M.M.; Murtala, A.; Lawal, M.; Mosa, A.A. Land degradation, causes, implications and sustainable management in arid and semi arid regions: A case study of Egypt. *Egypt. J. Soil Sci.* **2023**, *63*, 659–676. [CrossRef]
15. Abolhasani, A.; Zehtabian, G.; Khosravi, H.; Rahmati, O.; Alamdarloo, E.H.; D'Odorico, P. A new conceptual framework for spatial predictive modelling of land degradation in a semiarid area. *Land Degrad. Dev.* **2022**, *33*, 3358–3374. [CrossRef]
16. Fortesa Bernat, J. Assessing Temporal Variability and Controlling Factors on the Hydrosedimentary Response in Mediterranean Catchments. Ph.D. Thesis, Universitat de les Illes Balears, Palma, Spain, 2020.
17. AbdelRahman, M.A. An overview of land degradation, desertification and sustainable land management using GIS and remote sensing applications. *Rend. Lincei. Sci. Fis. E Nat.* **2023**, *34*, 767–808. [CrossRef]
18. Mohamed, E.S.; Belal, A.; Saleh, A. Assessment of land degradation east of the Nile Delta, Egypt using remote sensing and GIS techniques. *Arab. J. Geosci.* **2013**, *6*, 2843–2853. [CrossRef]
19. El Nahry, A.; Ibraheim, M.; El Baroudy, A. Assessment of soil degradation in the northern part of Nile Delta, Egypt, using remote sensing and GIS techniques. *Egypt. J. Remote Sens. Space Sci.* **2008**, *11*, 139–154.
20. Abowaly, M.E.; Ali, R.A.; Moghanm, F.S.; Gharib, M.S.; Moustapha, M.E.; Elbagory, M.; Omara, A.E.-D.; Elmahdy, S.M. Assessment of soil degradation and hazards of some heavy metals, using remote sensing and GIS techniques in the Northern part of the Nile Delta, Egypt. *Agriculture* **2022**, *13*, 76. [CrossRef]
21. Gad, A. Qualitative and quantitative assessment of land degradation and desertification in egypt based on satellite remote sensing: Urbanization, salinization and wind erosion. In *Environmental Remote Sensing in Egypt*; Springer: Cham, Switzerland, 2020; pp. 443–497.
22. Arnous, M.O.; Mansour, B.M. Utilizing multi-temporal thermal data to assess environmental land degradation impacts: Example from Suez Canal region, Egypt. *Environ. Sci. Pollut. Res.* **2023**, *30*, 2145–2163. [CrossRef]
23. El-Gammal, M.; Ali, R.; Abou Samra, R. GIS-based land degradation risk assessment of Damietta governorate, Egypt. *Egypt. J. Basic Appl. Sci.* **2015**, *2*, 183–189. [CrossRef]
24. El-Zeiny, A.; Gad, A.; El-Gammal, M.; Salem, M. Geospatial techniques for detection of vulnerable areas to contamination at Damietta coast, Nile Delta, Egypt. *J. Environ. Sci.* **2016**, *5*, 64–69.
25. Staff, S.S. Soil taxonomy: A basic system of soil classification for making and interpreting soil surveys. *Agric. Handb.* **1999**, *436*, 336–337.
26. Badawy, S.; El-Motaium, R.; El-Sayed, M.; Abdel-Lattif, H.; Ghorab, H.; Hossain, M. Environmental impact assessment of Egyptian Damietta governorate soils contamination with cadmium. *MOJ Eco. Environ. Sci* **2021**, *6*, 216–228.
27. EGPC/CONCO-Coral. *Geologic Map of Egypt, Scale 1:500000, Cairo, Egypt*; EGPC/CONCO-Coral: Cairo, Egypt, 1987.
28. FAO. *Guidelines for Soil Description*; FAO: Rome, Italy, 2006.
29. Soil Survey Staff. *Soil Survey Field and Laboratory Methods Manual. Soil Survey Investigations Report No. 51, Version 2.0. R. Burt and Soil Survey Staff (ed.)*; U.S. Department of Agriculture, Natural Resources Conservation Service: Washington, DC, USA, 2014.
30. Sandeep, P.; Reddy, G.O.; Jegankumar, R.; Arun Kumar, K. Modeling and assessment of land degradation vulnerability in semi-arid ecosystem of Southern India using temporal satellite data, AHP and GIS. *Environ. Model. Assess.* **2021**, *26*, 143–154. [CrossRef]
31. Kosmas, C.; Ferrara, A.M.S.; Briasouli, H.; Imeson, A. Methodology for mapping environmentally sensitive areas (ESAs) to desertification. In *The Medalus Project Mediterranean Desertification and Land Use. Manual on Key Indicators of Desertification and Mapping Environmentally Sensitive Areas to Desertification*; European Commission: Brussel, Belgium, 1999; pp. 31–47.
32. Sharma, T.; Singh, O. Soil erosion susceptibility assessment through geo-statistical multivariate approach in Panchkula district of Haryana, India. *Model. Earth Syst. Environ.* **2017**, *3*, 733–753. [CrossRef]
33. Soil Survey Staff. *Soil Survey Manual in USDA Handbook 18*; Ditzler, C., Scheffe, K., Monger, H.C., Eds.; U.S. Department of Agriculture, Natural Resources Conservation Service: Washington, DC, USA, 2017.
34. Fenta, A.A.; Tsunekawa, A.; Haregeweyn, N.; Poesen, J.; Tsubo, M.; Borrelli, P.; Panagos, P.; Vanmaercke, M.; Broeckx, J.; Yasuda, H. Land susceptibility to water and wind erosion risks in the East Africa region. *Sci. Total Environ.* **2020**, *703*, 135016. [CrossRef] [PubMed]
35. Abuzaid, A.S.; AbdelRahman, M.A.; Fadl, M.E.; Scopa, A. Land degradation vulnerability mapping in a newly-reclaimed desert oasis in a hyper-arid agro-ecosystem using AHP and geospatial techniques. *Agronomy* **2021**, *11*, 1426. [CrossRef]
36. Haghighi, A.T.; Darabi, H.; Karimidastenaei, Z.; Davudirad, A.A.; Rouzbeh, S.; Rahmati, O.; Sajedi-Hosseini, F.; Klöve, B. Land degradation risk mapping using topographic, human-induced, and geo-environmental variables and machine learning algorithms, for the Pole-Doab watershed, Iran. *Environ. Earth Sci.* **2021**, *80*, 1. [CrossRef]

37. AbdelRahman, M.A.E.; Tahoun, S. GIS model-builder based on comprehensive geostatistical approach to assess soil quality. *Remote Sens. Appl. Soc. Environ.* **2019**, *13*, 204–214. [CrossRef]
38. Parmar, M.; Bhawsar, Z.; Kotecha, M.; Shukla, A.; Rajawat, A.S. Assessment of land degradation vulnerability using geospatial technique: A case study of Kachchh District of Gujarat, India. *J. Indian Soc. Remote Sens.* **2021**, *49*, 1661–1675. [CrossRef]
39. López, M.; de Dios Herrero, J.; Hevia, G.G.; Gracia, R.; Buschiazzo, D.E. Determination of the wind-erodible fraction of soils using different methodologies. *Geoderma* **2007**, *139*, 407–411. [CrossRef]
40. Awadhwal, N.; Thierstein, G. Soil crust and its impact on crop establishment: A review. *Soil Tillage Res.* **1985**, *5*, 289–302. [CrossRef]
41. Wang, G.; Wente, S.; Gertner, G.; Anderson, A. Improvement in mapping vegetation cover factor for the universal soil loss equation by geostatistical methods with Landsat Thematic Mapper images. *Int. J. Remote Sens.* **2002**, *23*, 3649–3667. [CrossRef]
42. Nakae, H.; Inui, R.; Hirata, Y.; Saito, H. Effects of surface roughness on wettability. *Acta Mater.* **1998**, *46*, 2313–2318. [CrossRef]
43. Ramón-Torregrosa, P.; Rodríguez-Valverde, M.; Amirfazli, A.; Cabrerizo-Vílchez, M. Factors affecting the measurement of roughness factor of surfaces and its implications for wetting studies. *Colloids Surf. A Physicochem. Eng. Asp.* **2008**, *323*, 83–93. [CrossRef]
44. Zhen, J.; Pei, T.; Xie, S. Kriging methods with auxiliary nighttime lights data to detect potentially toxic metals concentrations in soil. *Sci. Total Environ.* **2019**, *659*, 363–371. [CrossRef]
45. Aldabaa, A.A.A.; Yousif, I.A.H. Geostatistical approach for land suitability assessment of some desert soils. *Egypt. J. Soil Sci.* **2020**, *60*, 195–209. [CrossRef]
46. Mousavifard, S.M.; Momtaz, H.; Sepehr, E.; Davatgar, N.; Sadaghiani, M.H.R. Determining and mapping some soil physico-chemical properties using geostatistical and GIS techniques in the Naqade region, Iran. *Arch. Agron. Soil Sci.* **2013**, *59*, 1573–1589. [CrossRef]
47. Hilal, A.; Bangroo, S.A.; Kirmani, N.A.; Wani, J.A.; Biswas, A.; Bhat, M.I.; Farooq, K.; Bashir, O.; Shah, T.I. Geostatistical modeling—A tool for predictive soil mapping. In *Remote Sensing in Precision Agriculture*; Elsevier: Amsterdam, The Netherlands, 2024; pp. 389–418.
48. Oliver, M.; Webster, R. A tutorial guide to geostatistics: Computing and modelling variograms and kriging. *Catena* **2014**, *113*, 56–69. [CrossRef]
49. Ågren, A.; Lidberg, W.; Strömgren, M.; Ogilvie, J.; Arp, P. Evaluating digital terrain indices for soil wetness mapping—A Swedish case study. *Hydrol. Earth Syst. Sci.* **2014**, *18*, 3623–3634. [CrossRef]
50. FAO. *A Provisional Methodology for Soil Degradation Assessment*; FAO: Rome, Italy, 1980.
51. Soil Science Division Staff. *Soil Survey Manual. USDA Handbook 18*; Government Printing Office: Washington, DC, USA, 2017.
52. Richardson, C.; Sadler, T. Evaluating wind erosion sensitivity for landfill sites in New Mexico using fuzzy analytical hierarchy process (FAHP). *Am. J. Civ. Eng* **2022**, *10*, 1–12. [CrossRef]
53. Abd-Elazem, A.H.; El-Sayed, M.A.; Fadl, M.E.; Zekari, M.; Selmy, S.A.; Drosos, M.; Scopa, A.; Moursy, A.R. Estimating Soil Erodible Fraction Using Multivariate Regression and Proximal Sensing Data in Arid Lands, South Egypt. *Soil Syst.* **2024**, *8*, 48. [CrossRef]
54. Masri, Z.; Van Donk, S.; Bruggeman, A.; Turkelboom, F. Post-harvest summer tillage to control wind erosion in the Khanasser Valley, Syria. *Aeolian Res.* **2015**, *17*, 219–229. [CrossRef]
55. Song, W.; Mu, X.; Ruan, G.; Gao, Z.; Li, L.; Yan, G. Estimating fractional vegetation cover and the vegetation index of bare soil and highly dense vegetation with a physically based method. *Int. J. Appl. Earth Obs. Geoinf.* **2017**, *58*, 168–176. [CrossRef]
56. Shao, W.; Wang, Q.; Guan, Q.; Zhang, J.; Yang, X.; Liu, Z. Environmental sensitivity assessment of land desertification in the Hexi Corridor, China. *Catena* **2023**, *220*, 106728. [CrossRef]
57. Abdel-Raheem, K.H.; Khalil, M.M.; Abdelhady, A.A.; Tan, L. Anthropogenic–induced environmental and ecological changes in the Nile Delta over the past half-century. *Sci. Total Environ.* **2024**, *926*, 171941. [CrossRef] [PubMed]
58. Grall, C.; Steckler, M.; Pickering, J.; Goodbred, S.; Sincavage, R.; Paola, C.; Akhter, S.; Spiess, V. A base-level stratigraphic approach to determining Holocene subsidence of the Ganges–Meghna–Brahmaputra Delta plain. *Earth Planet. Sci. Lett.* **2018**, *499*, 23–36. [CrossRef]
59. Arnous, M.O.; Hegazi, A.M.; El-Rayes, A.E.; Almoazamy, A.A. Identification of geomorphic signatures of active tectonics in the Wadi Hagul Basin, Northwest Gulf of Suez, Egypt: Insights from SRTM derived geomorphic indices and watershed analysis. *J. Coast. Conserv.* **2023**, *27*, 40. [CrossRef]
60. Zhu, X.; He, H.S.; Zhang, S.; Dijak, W.D.; Fu, Y. Interactive effects of climatic factors on seasonal vegetation dynamics in the Central Loess Plateau, China. *Forests* **2019**, *10*, 1071. [CrossRef]
61. Guan, Q.; Feng, L.; Tang, J.; Park, E.; Ali, T.A.; Zheng, Y. Trends in river total suspended sediments driven by dams and soil erosion: A comparison between the Yangtze and Mekong rivers. *Water Resour. Res.* **2022**, *58*, e2022WR031979. [CrossRef]
62. Yunus, A.P. Geomorphic and lithologic control on bedrock channels in drainage basins of the Western Arabian Peninsula. *Arab. J. Geosci.* **2016**, *9*, 133. [CrossRef]

63. Gad, A.; Mansour, R. Index integrating soil, vegetation, climate and management qualities to evaluate desertification in the Northwestern coast, Egypt. *Int. J. Environ. Eng. Dev* **2023**, *1*, 250–265. [CrossRef]
64. Mohammed, H.; Hansen, A.T. Spatial heterogeneity of low flow hydrological alterations in response to climate and land use within the Upper Mississippi River basin. *J. Hydrol.* **2024**, *632*, 130872. [CrossRef]
65. Daniela, R.; Marco, V. Land use and landscape pattern changes driven by land reclamation in a coastal area: The case of Volturno delta plain, Campania Region, southern Italy. *Environ. Earth Sci.* **2017**, *76*, 694. [CrossRef]
66. Saeed, M.; Khafagi, O.; Bedair, R. Soil Quality Assessment for Wheat Cultivation in El–Menoufia Governorate, Nile Delta, Egypt. *J. Soil Sci. Agric. Eng.* **2018**, *9*, 693–698. [CrossRef]
67. Menon, M.; Sarkar, B.; Crotty, F.; Whalley, R.; Ludwig, B. Editorial for the special issue on 'Opportunities and Challenges in No-Till Farming'. *Eur. J. Soil Sci.* **2020**, *71*, 971–973. [CrossRef]
68. Cassol, C.; Conceição, P.C.; Amadori, C.; Haskel, M.K.; Freitas, L.A.d.; Tomazoni, A.R. Residual biomass quality index: A tool for conservation agriculture. *Rev. Bras. Ciência Solo* **2023**, *47*, e0220150. [CrossRef]
69. Nunes, A.L.; Bartz, M.L.; Mello, I.; Bortoluzzi, J.; Roloff, G.; Fuentes Llanillo, R.; Canalli, L.; Wandscheer, C.A.; Ralisch, R. No-till System Participatory Quality Index in land management quality assessment in Brazil. *Eur. J. Soil Sci.* **2020**, *71*, 974–987. [CrossRef]
70. Masto, R.; Chhonkar, P.; Purakayastha, T.; Patra, A.; Singh, D. Soil quality indices for evaluation of long-term land use and soil management practices in semi-arid sub-tropical India. *Land Degrad. Dev.* **2008**, *19*, 516–529. [CrossRef]
71. Elbasiouny, H. Assessment of environmental sensitivity to desertification, soil quality and sustainability in an area of the North Nile Delta, Egypt. *Egypt. J. Soil Sci.* **2018**, *58*, 399–415. [CrossRef]
72. Abdel-razek, M.A. Soil Quality as Indicated by Physical and Chemical Properties in Some Tanta Areas, Nile Delta, Egypt Using Remote Sensing and GIS Techniques. *Ann. Agric. Sci. Moshtohor* **2021**, *59*, 747–760. [CrossRef]
73. Ladisa, G.; Todorovic, M.; Liuzzi, G.T. A GIS-based approach for desertification risk assessment in Apulia region, SE Italy. *Phys. Chem. Earth Parts A/B/C* **2012**, *49*, 103–113. [CrossRef]
74. Gabriele, M.; Brumana, R.; Previtali, M.; Cazzani, A. A combined GIS and remote sensing approach for monitoring climate change-related land degradation to support landscape preservation and planning tools: The Basilicata case study. *Appl. Geomat.* **2023**, *15*, 497–532. [CrossRef]

Disclaimer/Publisher's Note: The statements, opinions and data contained in all publications are solely those of the individual author(s) and contributor(s) and not of MDPI and/or the editor(s). MDPI and/or the editor(s) disclaim responsibility for any injury to people or property resulting from any ideas, methods, instructions or products referred to in the content.